JOURNAL OF MATERIALS SCIENCE **37** (2002) 1173–1178

Structure and properties of AlMgSi1 alloy tailored for semi-solid forming

HEIMO WABUSSEG, GIAN-CARLO GULLO, PETER J. UGGOWITZER
Insitute of Metallurgy, ETH Zentrum, CH-8092 Zurich, Switzerland
E-mail: wabusseg@met.mat.ethz.ch; gullo@met.mat.ethz.ch; uggo@met.mat.ethz.ch

KURT STEINHOFF
Department of Production Engineering and Industrial Organisation, TU Delft, NL-2628 CD Delft, The Netherlands
E-mail: k.steinhoff@wbmt.tudelft.nl

HELMUT KAUFMANN
Leichtmetallkompetenzzentrum Ranshofen GmbH (LKR), A-5282 Ranshofen, Austria
E-mail: helmut.kaufmann@arcs.ac.at

Thixoforming requires semi-solid slurries, which contain a high volume fraction of non-dendritic solid phase with special grain morphology. Volume fraction, geometry and connectivity of the solid α-phase has to be kept within narrow limits. The paper illustrates the development of a new aluminium based wrought alloy AlMgSi1 alloy, adapted with barium, characterised by a microstructure which exhibits a low sensitivity towards fluctuations in process parameters resulting in improved mechanical properties of the alloy. The rheological behaviour of the new alloy by means of backward extrusion experiments is described, and an overview of the static and dynamic strength properties is given that can be achieved when the alloy is processed by means of the New Rheocasting process.

1. Introduction

The discovery of shear rate dependent viscosity for metals in the solidification range in the early 1970s [1] was the starting point for the development of semi-solid processing routes. In the past 30 years a number of processes named Thixocasting, Thixoforging, semi-liquid Casting and Rheocasting, have advanced to becoming manufacturing routes of industrial relevance.

The key feature of all these processes is the specific flow behaviour of semi-solid slurries, which contain a high volume fraction of non-dendritic solid phase. Such a semi-solid slurry allows a laminar, smooth front filling of the die, thanks to the increased viscosity compared with fully liquid melts. Since air entrapment can be avoided heat treatable and weldable components with low porosity levels are obtained, which are superior in mechanical properties compared to conventional die-casting parts. Additionally, the die filling temperature as well as the heat content of the metal are lower, leading to longer die life and higher productivity. Semi-solid processes are near-net shape forming technologies. Compared with conventional casting and forging processes the machining cost can be reduced. Due to these advantages semi-solid cast and forged parts have replaced conventional forgings, permanent mould and investment castings, and in some instances even die castings. Applications include automotive suspension parts, wheels, master brake cylinders, antilock brake valves, pump housings, electrical connector multiconductors, brass plumbing components and many more parts covering the field of automotive, aerospace and mechanical engineering components.

However, a wider technical implementation of semi-solid forming in large scale production requires improved stability of the process and high reproducibility of product quality. The classical processing routes for semi-solid forming comprise the production of precursor material with globular α-phase and the reheating of the slugs into the semi-solid state by induction heating, followed by casting or forging of the latter into shape in High Pressure Die Casting machines (HPDC) or in forging presses.

For a given alloy the required flow characteristics and product properties can only be achieved within a narrow temperature window and at special grain morphologies of the microstructure. This requires precise process control.

Depending on the diameter of the slugs, the reheating time can vary from 5 minutes up to more than 20 minutes. After this heating period the temperature distribution along the cross-section and over the whole length of the semi-solid slugs must be uniform. Small temperature fluctuations may lead to unsuitable amounts of liquid fraction and thus result in unfavourable semi-solid forming conditions. In particular, for wrought alloys the semi-solid processing range

is difficult to adjust due to the high sensitivity to the liquid volume fraction on temperature changes. Therefore, a precise and usually long homogenisation time is necessary in order to obtain a uniform temperature distribution over the cross section of the semi-solid slug. However, in most cases this leads to grain coarsening and grain coalescence and, consequently, to the deterioration of the rheological and flow properties.

It was the main target of the research work presented in this paper to design an aluminium wrought alloy tailored specifically for semi-solid forming. The inherent properties of this alloy should help to stabilise the process and make it less prone to fluctuations in the processing parameters. The adapted alloy should be less sensitive (i) to long holding times within the semi-solid state and (ii) to variations in the solid/liquid volume fraction, thus permitting a better control of the process.

In the following the microstructural features of two AlMgSi1 (AA6082) alloys in the semi-solid state are discussed in detail. A recently developed AlMgSi1 alloy modified with barium and optimised for the semi-solid forming process is compared to a standard AlMgSi1. Grain growth and grain coalescence as a function of different solid/liquid fractions and holding periods are considered. In order to describe the solid-skeleton changes, particular attention is paid to the variation of the contiguity of the solid phase and its effect on the thixotropic flow characteristic. Furthermore, microstructural evolution, flow characteristics and mechanical properties are presented.

2. Experimental procedure

2.1. Materials

Different grades of semi-solid precursor materials of AlMgSi1 alloys were used for quenching, backward extrusion and casting experiments. The chemical compositions are given in Table I. Continuously cast rods of diameter 80 mm in MHD-stirred condition were supplied by the company SAG, Austria. While alloy 1 was a conventional AlMgSi1 grade, alloy 2 has been modified with barium.

2.2. Quenching experiments

The microstructural evolution in the semi-solid state was investigated by using cubic samples of 10 mm side length. The specimens were cut from the precursor rods and partially re-melted to various solid/liquid fractions in a vertical IR tube furnace and held at various semi-solid temperatures and homogenisation times before water quenching. After polishing and etching, the microstructure was characterised by means of light optical image analysis in order to determine the relevant microstructural parameters.

TABLE I Chemical compositions of alloy 1 and 2 (weight-percent)

	Si	Mg	Mn	Fe	Cr	Cu	Ti	Zr	Ba	Rest
Alloy 1	1.00	0.69	0.42	0.23	0.11	0.05	0.07	<0.01	–	<0.02
Alloy 2	1.02	0.67	0.40	0.23	0.11	0.04	0.06	<0.01	0.2	<0.02

2.3. Backward extrusion experiments

The rheological properties of the re-melted alloy were studied by means of backward extrusion experiments. Cylindrical specimens (26 mmØ × 35 mm long) were heated and partially re-melted in a steel container, using the same vertical IR tube furnace as for quenching experiments. After homogenisation times of 5, 10, 20 and 30 minutes, respectively, the specimens were isothermally backwards extruded around the stationary plunger at constant ram speed. The chosen ram speed was 200 mm/s (shear rate 70 s^{-1}), which represents a good approximation to industrial shear rates. Ram displacement and extrusion forces were measured. Details of the experiment are described elsewhere [2].

2.4. Casting experiments and mechanical tests

In the casting experiments the same alloys were taken in fully liquid state from a melting and holding furnace, poured into steel cups and transformed into semi-solid slugs of 80 mm diameter and 120 mm length by means of the New Rheocasting (NRC) technique [3]. The melt temperature in the holding furnace was 665°C (only about 15°C above liquidus temperature), whereas the forming temperature was 642°C, corresponding to liquid fractions of about 45%. These slugs were then transferred into the sleeve of an UBE HVSC 350 Squeeze Casting machine and cast into a 4-step die (step wall thickness 14 mm, 10 mm, 6 mm and 2 mm). The die temperature was held constant at a level of 270°C. The step plate castings were then heat treated to peak hardness. This T6 heat-treatment was performed at 540°C for 5 hours, followed by water quenching and artificial ageing at 170°C for 10 hours.

Round tensile test specimens of 4 mm diameter were taken from the steps with 14 mm, 10 mm, and 6 mm thickness and tested in the T6 condition at room temperature. Cylindrical hourglass-shaped fatigue strength test specimens, with a minimum diameter of 6 mm, were taken from the two thickest steps, and tested in the T6 condition with $R = 0.1$ and $f = 50$ Hz at room temperature on a servo-hydraulic tensile/compression test machine.

3. Microstructure and flow characteristics

The conventional semi-solid forming processes, such as Thixocasting or Thixoforging, are based on the fact that in the un-perturbed state the semi-solid slugs can be handled like solid rods, but attain fluid-like properties during shearing. It is generally accepted that the solid-like characteristic is due to the presence of a solid skeleton consisting of interconnected grains. During the forming operation the bonds between grains break under shear stress, resulting in a significant decrease of viscosity [1, 4, 5].

A useful microstructural parameter describing the magnitude of the solid skeleton is the contiguity of the solid phase C^{α} [6, 7]. The contiguity is a measure for the amount of solid-solid contact in a semi-solid structure and is defined as the average fraction of the surface

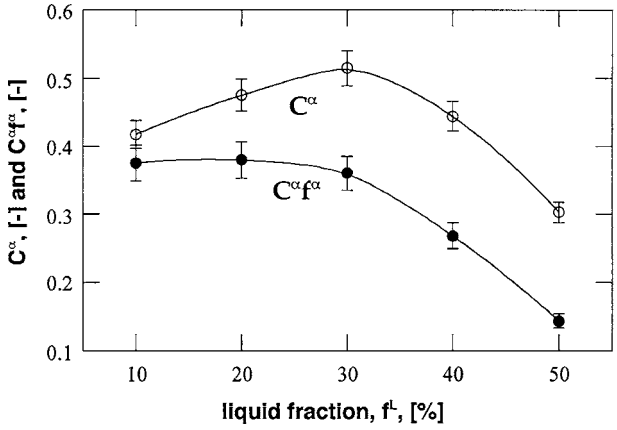

Figure 1 Contiguity C^{α} (○) and contiguity volume $C^{\alpha} f^{\alpha}$ (●) vs. liquid fraction at an isothermal holding time of 5 min.

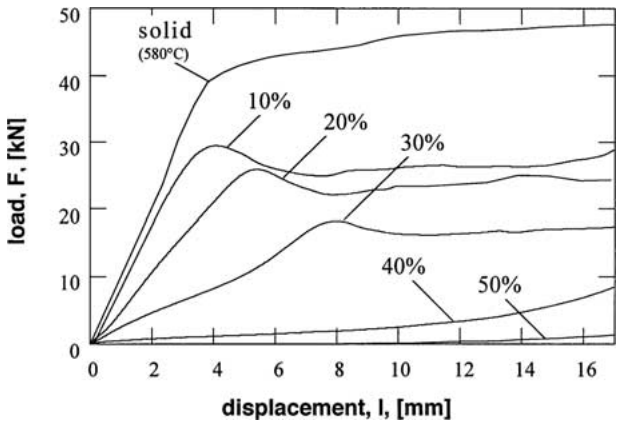

Figure 2 Extrusion curves for alloy 1 at different liquid fractions ($0 < f^{L} < 0.5$). Isothermal holding time 5 min, ram speed 200 mm/s.

area shared by one grain with all neighbouring grains of the same phase, $C^{\alpha} = 2S^{\alpha\alpha}/(2S^{\alpha\alpha} + S^{\alpha L})$, with $S^{\alpha\alpha}$ being the $\alpha\alpha$-grain boundary and $S^{\alpha L}$ being the boundary between α-Al and the liquid phase. Contiguity is a parameter, which quantitatively helps to describe the distribution of phases in coarse two-phase alloys. For alloys in the semi-solid state, it is appropriate to standardise the contiguity by multiplying it by the fraction of solid, f^{α}, hence the contiguity volume $C^{\alpha} f^{\alpha}$, which quantifies the connecting portion of the solid phase [8]. Fig. 1 illustrates the decreasing contiguity volume with increasing liquid fractions up to 50% f^{L}. Fig. 2 shows the effect of the liquid fraction f^{L} on the flow characteristics, measured by backward extrusion, for alloy 1 as a function of temperature.

In the fully solid state ($C^{\alpha} f^{\alpha} = 1$) the alloy shows a typical hot forming flow characteristic with a steep increase of the force at small displacements (elastic range) followed by deformation of the specimen before reaching a steady-state plateau. A similar behaviour is observed for specimens with liquid fractions f^{L} lower than 30%. In this range of liquid fractions, the bridging of the solid skeleton is highly pronounced, and the contiguity volume $C^{\alpha} f^{\alpha}$ exceeds 0.3. The microstructural examination of the deformed specimens after backward extrusion revealed an expulsion of the liquid phase and a corresponding densification of the solid at the bottom of the container, as reported by Loué *et al.* [2]. This

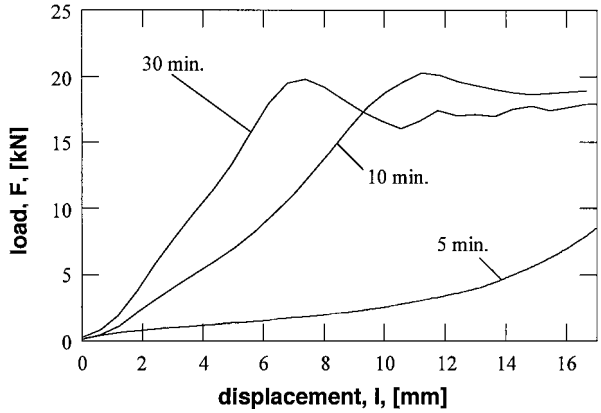

Figure 3 Extrusion curves for alloy 1 as a function of the isothermal holding at a constant liquid fraction of 40%, ram speed 200 mm/s.

suggests that the deformation process is essentially confined to the skeleton. Extensive disruption of the solidly bound particles does not take place and therefore, no thixotropic behaviour is observed [5].

At liquid fraction levels of $f^{L} = 0.4$ and 0.5, on the other hand, the slugs are sufficiently stable to maintain their cylindrical shape, but deform without any remarkable increase in force, indicating that the contiguity volume is low enough to permit the required disruption of the bridges between solid grains. Consequently, the flow characteristic can be assumed to be thixotropic at $C^{\alpha} f^{\alpha} < 0.3$ (Fig. 1).

For contiguity volume levels below 0.1 at $f^{L} > 0.6$ very low extrusion forces are measured, because the solid-phase particles are only weakly inter-connected in a 3D network and the billet becomes unstable and looses its shape stability. The fact that a contiguity volume $C^{\alpha} f^{\alpha}$ of 0.3 describes a pragmatic upper limit for the solid skeleton's cohesion will be discussed further below.

Fig. 3 illustrates the measured force during backward extrusion for different holding periods at a constant liquid fraction of 40%. It is apparent that after exceeding 5 minutes isothermal holding time, the behaviour of alloy 1 shifts from a homogeneous, thixotropic shear deformation to an unfavourable elastoplastic deformation. Obviously, longer homogenisation times lead to an increase in the flow resistance of alloy 1. The reason for the drastically different rheological behaviour is attributed to the microstructural change of the semi-solid alloy during isothermal holding, mainly involving an increase of the contiguity volume. As will be shown later, both spheroidisation and particle size increase with longer homogenisation times, which in turn also affect the contiguity. As soon as the coarsening grains start contacting each other they interconnect via solid neck bonds [9, 10]. This coalescence phenomenon influences the cohesion and interlocking of the solid skeleton, hence the rheological behaviour of the alloy [11].

An effective way of reducing the contiguity growth rate of the solid skeleton is offered by the enhanced wetting properties [5, 12] between the α-phase and the remaining liquid, as indicated schematically in Fig. 4. The contiguity of the solid phase is affected by the relative

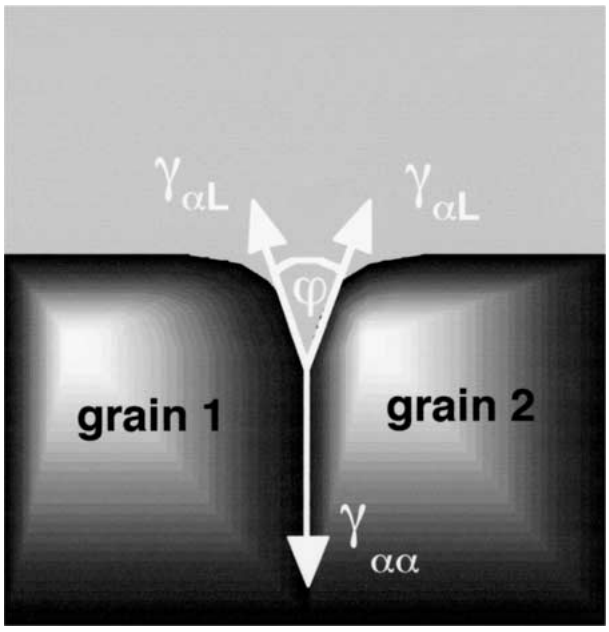

Figure 4 Schematic image of liquid penetration between two adjacent grains. Note that solid grains are less connected at lower $\gamma_{\alpha L}$-values.

values of the solid/solid and solid/liquid interface energies. Therefore, two adjacent grains will become contiguous if the condition $\gamma_{\alpha\alpha} < 2\gamma_{\alpha L}$ is fulfilled, where $\gamma_{\alpha\alpha}$ is the energy of the contiguous solid/solid boundary and $\gamma_{\alpha L}$ is the energy of the solid/liquid interface. The lower the value of the solid/liquid interface energy $\gamma_{\alpha L}$ is, relative to $\gamma_{\alpha\alpha}$, the more pronounced is the penetration of the liquid between the grains and, consequently, the lower will be the contiguity and the strength of the solid bonds. Furthermore, the solid/liquid interface energy $\gamma_{\alpha L}$ is the driving force for the spheroidisation and the growth of the solid phase.

It was found that small amounts of barium diminish the solid/liquid interface energy $\gamma_{\alpha L}$ [12] and consequently increase the penetration of the liquid phase between the α-Al grains, which in turn lead to lower contiguity values C^{α}. Small additions of barium result in a decrease of $\gamma_{\alpha L}$, therefore reducing the α-Al grain growth and, due to the abated spheroidisation, increasing the shape factor F^{α} (note: shape factor $F^{\alpha} = (S^{\alpha L})^2/4\pi A^{\alpha}$, with A^{α} as average area of α-Al grains and $S^{\alpha L}$ being the length of the α-liquid phase boundary; normally F^{α} is >1, however in case of fully spherical grains F^{α} is equal to 1).

Fig. 5 indicates the flow characteristic of the new barium-containing alloy 2 during isothermal holding at a constant liquid fraction of $f^{L} = 40\%$. It shows practically no increase in flow resistance even after 30 min holding time. This can be attributed to the favourable behaviour during homogenisation.

As shown in Fig. 6, the contiguity volume of the solid phase remains in the range of 0.2 to 0.25 and does not exceed the critical value of 0.3, thus forming a weakly interconnected solid skeleton. On the other hand, the contiguity volume of alloy 1 exceeds a value of 0.3 and loses its shear thinning behaviour (see Fig. 3).

As mentioned above, the low cohesion of the solid network in alloy 2 is due to the increased penetration of the liquid phase between the grain contacts

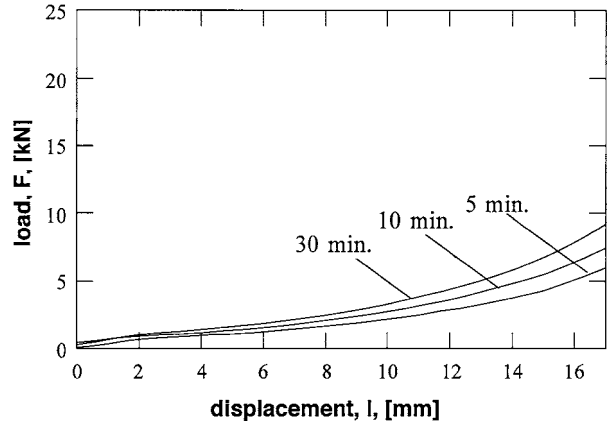

Figure 5 Extrusion curves for alloy 2 as a function of the isothermal holding time at a constant liquid fraction of 40%, ram speed 200 mm/s.

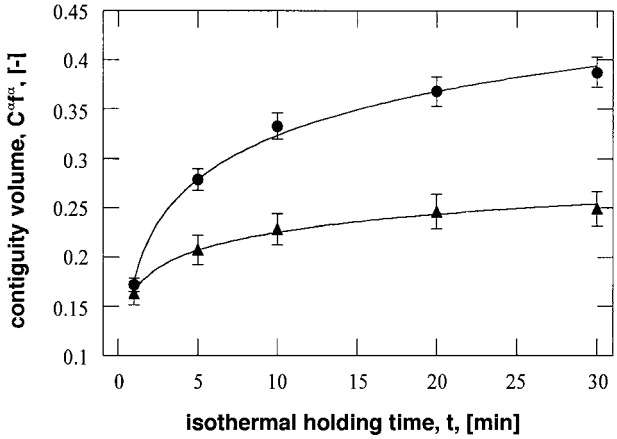

Figure 6 Contiguity volume $C^{\alpha}f^{\alpha}$ vs. isothermal holding time for alloy 1 (●) and alloy 2 (▲) at 40% liquid fraction.

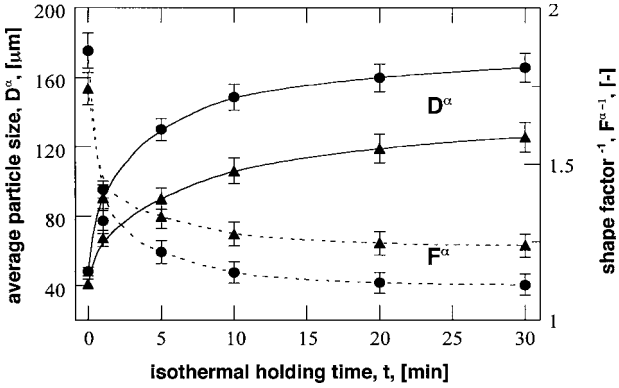

Figure 7 D^{α} and F^{α} vs. isothermal holding time for alloy 1 (●) and alloy 2 (▲) at 40% liquid fraction.

and the reduced grain coarsening attained by the effect of barium in reducing the interface energy $\gamma_{\alpha L}$ (Fig. 7). The weakly interconnected solid skeleton changes only slightly with increasing holding times, consequently allowing a homogeneous deformation of the semi-solid slug even after longer homogenisation times.

From Figs 6 and 7 it becomes obvious that the alloy composition affects the isothermal-coarsening rate. Due to the difference in the driving force, namely the interface energy $\gamma_{\alpha L}$, the coarsening rate for the particles decreases from alloy 1 to alloy 2 (both had initial grain sizes close to 50 μm). It is generally accepted, that

the cavity filling behaviour is better with smaller grain sizes, especially for thin wall sections and therefore, the Ba modified alloy 2 is of advantage.

4. Mechanical properties

Fig. 8 shows the yield strength $R_{p0.2}$, the ultimate tensile strength R_m and the elongation to fracture A_5 for alloys 1 and 2 in T6 condition. All data are mean values of at least 12 specimens tested for each alloy. A yield strength level of approximately 320 MPa and a fracture elongation of >3% can be achieved if suitable process parameters are chosen. No significant difference between alloy 1 and alloy 2 can be recognised. The strength properties are satisfactory and are close to forging qualities. Note that the DIN1749 standard for die forged components request a minimum value of 260 MPa for $R_{p0.2}$ and 310 MPa for R_m, respectively, which is clearly exceeded by the NRC properties presented here. The required elongation to fracture of 6% for forged AlMgSi1, however, cannot be reached. The gap must be due to the fact that at least the initial liquid portion of the alloy solidifies in non-equilibrium, which results in the formation of undesired secondary phases [13].

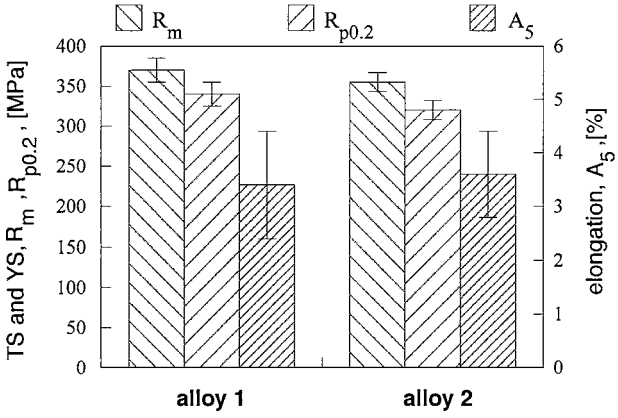

Figure 8 Mechanical properties (yield strength, $R_{P0.2}$, ultimate tensile strength, R_m, and elongation to fracture, A_5) of alloy 1 and 2 in T6 condition.

Figs 9 and 10 illustrate typical sections of the microstructure of alloy 1 and alloy 2, respectively. It is clear that the structure of both alloys is characterised by the presence of secondary phases. Alloy 1 features local liquid pocket segregations with needle shaped silicon ("non-equilibrium eutectic" due to non-equilibrium solidification), which is accompanied by polygonal α-(AlFeSi) compounds, where Fe is partly substituted

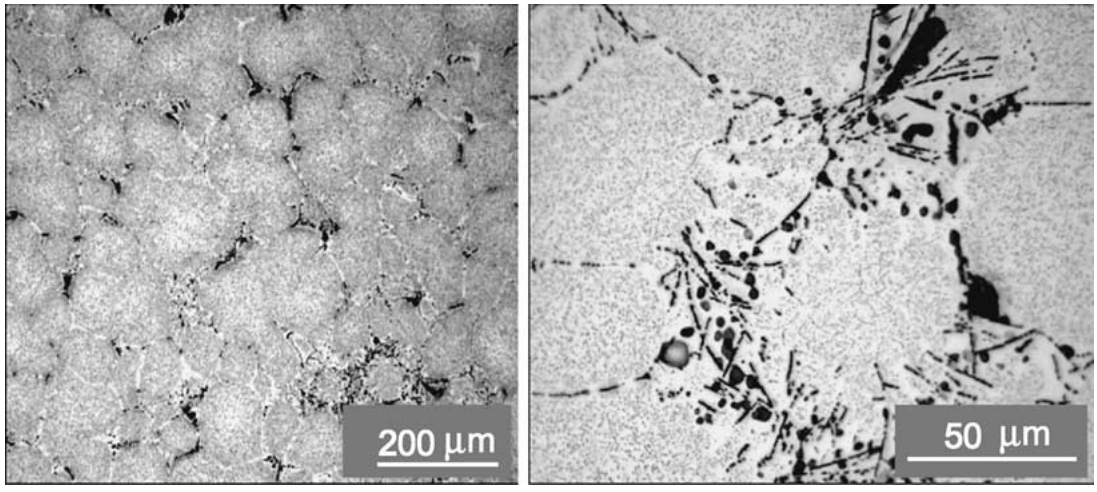

Figure 9 Microstructure of alloy 1 in T6 condition, characterized by the presence of secondary phases along grain boundary. Sections of liquid pocket segregation (right) show pronounced formation of needle shaped Si and α-(AlFeSi) compounds.

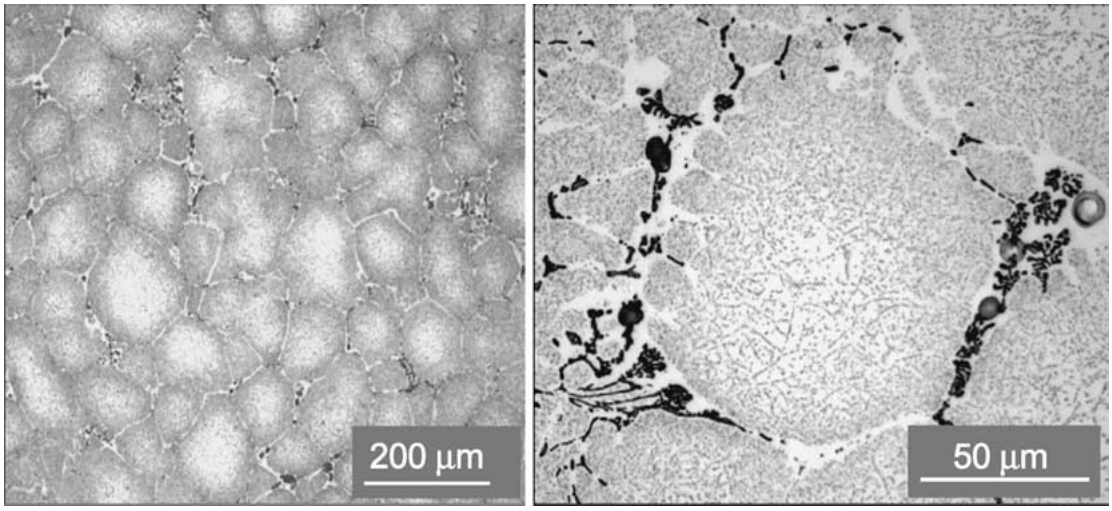

Figure 10 Microstructure of alloy 2 in T6 condition. Compared to alloy 1 the secondary Si-phase is more rounded and rosette-like shaped.

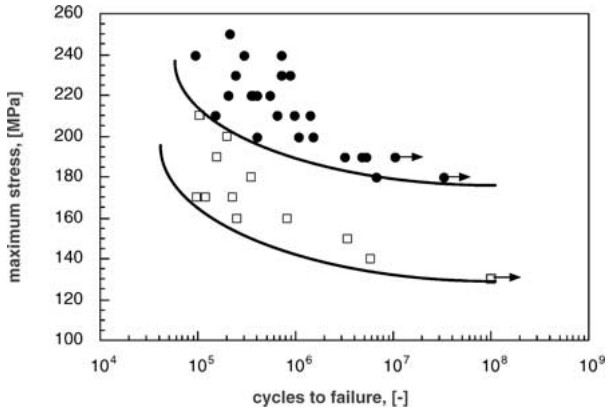

Figure 11 Fatigue strength data for the 14 mm and 10 mm plates of the 4-step die in the T6 condition for alloy 1 (□) and alloy 2 (●). $R = 0.1$.

by manganese. The microstructure of alloy 2 exhibits more rounded and rosette-like shaped phases along the grain boundaries. According to EDX-measurements these phases are of the same composition as the Si and α-phases; additionally a strong barium signal is obtained. The morphology of the secondary phases indicates that barium might also act as a modifying element. Lu and Hellawell [14] reported that elements such as barium modify the eutectic silicon flakes in aluminium-silicon cast alloys to branched fibres with high twin densities, and primary flakes to nearly spherical shapes.

Although the effect of barium addition on the morphology of the secondary phases does not significantly affect the static mechanical properties, a significant influence on the dynamic properties is observed. Fig. 11 shows the results of the fatigue tests. The Bamodified alloy 2 exhibits significantly higher fatigue strength values.

In alloy 1, the needle-shaped eutectic Si particles, which are up to 30 μm long, may act as crack initiation sites and may reduce the fatigue strength, whereas crack nucleation at the rounded phases in alloy 2 is assumed to be less dominant.

5. Conclusions

In this paper it is shown that small additions of barium to a standard AlMgSi1 alloy have positive effects on formability and product quality in semi-solid forming. Primarily, Ba reduces the solid/liquid interface energy $\gamma_{\alpha L}$, which enhances wetting between the α-Al grains and the remaining liquid in a semi-solid slug. This reduces the contiguity growth rate of the solid phase during holding in the solidification range. The alloy maintains good flow properties even after extended periods of holding at higher temperatures. $\gamma_{\alpha L}$ is also the driving force for the spheroidisation and the growth of the solid phase. Starting from same shape factors in the precursor material, the α-Al phase in the barium-containing alloy does not spheroidise as quickly, as in the barium-free alloy. This is a slight disadvantage, but F^{α} remained in the positive range at all holding times tested in the experiments presented. The grain size, on the other hand, does not grow as fast, which is beneficial for semi-solid forming.

Barium-containing alloy AlMgSi1 gives definitely more flexibility to the manufacturer of semi-solid formed parts, because of a much wider processing window in terms of time. An additional improvement was found during fatigue testing: barium acts as a modifier for the Si-phase in the alloy and, therefore, increases the fatigue limit compared to barium free AlMgSi1.

Acknowledgment

H. W., H. K. und P. J. U. thank the Technologie Impulse GmbH (TIG) and the State of Upper Austria for supporting this work in the frame of the Kplus—Programme at LKR. G.-C. G. and K. S. thank the SM AG Altdorf, Switzerland for financial support.

References

1. M. C. FLEMINGS, *Metall. Trans.* A **22A** (1991) 957.
2. W. R. LOUE, M. SUERY and J. L. QUERBES, in Proc. 2nd Int. Conf. Semi-Solid Alloys, MIT, June 1992, p. 266.
3. H. KAUFMANN, M. NAKAMURA, H. WABUSSEG and P. J. UGGOWITZER, *Diecasting World* **174** (2000) 14.
4. P. KAPRANOS, in Proc. EUROMAT 1989 Conf., DGM, Aachen, 1989, p. 165.
5. D. H. KIRKWOOD, *Int. Mater. Rev.* **39**(5) (1994) 173.
6. E. E. UNDERWOOD, in "Quantitative Stereology" (Addison-Wesley, Reading, MA, 1970) p. 103.
7. H. KAUFMANN, H. WABUSSEG and P. J. UGGOWITZER, *Aluminium* **76** (1/2) (2000) 70.
8. H. C. LEE and J. GURLAND, *Mat. Sci. Eng*. **33** (1978) 125.
9. G. WAN and P. R. SAHM, in Proc. 2nd Int. Conf. Semi-Solid Alloys, MIT, June 1992, p. 328.
10. S. SANNES, H. GJESTLAND, L. ARNBERG and J. K. SOLBERG, in Proc. 3rd Int. Conf. Semi-Solid Alloys, Tokyo, June 1994, p. 75.
11. G. C. GULLO, K. STEINHOFF and P. J. UGGOWITZER, in Proc. 6th Int. Conf. Semi-Solid Alloys and Composites, Torino, September 2000, p. 367.
12. G. LANG, *Aluminium* **11** (1974) 731.
13. H. WABUSSEG, G. C. GULLO, H. KAUFMANN and P. J. UGGOWITZER, in Proc. 2nd Int. Conf. Processing Materials for Properties, San Francisco, November 2000, p. 37.
14. S.-Z. LU and A. HELLAWELL, *JOM* (1995) 38.

Received 14 February
and accepted 21 November 2001